Catalysis Today 266 (2016) 205–211

Contents lists available at ScienceDirect

Catalysis Today

journal homepage: www.elsevier.com/locate/cattod

The role of catalase and H_2O_2 in photocatalytic inactivation of *Escherichia coli*: Genetic and biochemical approaches

Minghui Gao[a,1], Tsz Wai Ng[a,1], Taicheng An[b,*], Guiying Li[b], Ho Yin Yip[a], Huijun Zhao[c], Po Keung Wong[a,**]

[a] School of Life Sciences, The Chinese University of Hong Kong, Shatin, NT, Hong Kong SAR, China
[b] State Key Laboratory of Organic Geochemistry, Guangzhou Institute of Geochemistry, Chinese Academy of Sciences, Guangzhou 510640, China
[c] Centre for Clean Environment and Energy, Griffith School of Environment, Gold Coast Campus, Griffith University, Queensland 4222, Australia

ARTICLE INFO

Article history:
Received 13 April 2015
Received in revised form
16 September 2015
Accepted 6 November 2015
Available online 21 December 2015

Keywords:
Photocatalytic inactivation
Single-gene deletion mutant
Catalase
H_2O_2
Photogenerated e^-

ABSTRACT

This study employed two different approaches, the inactivation of *Escherichia coli* single-gene deleted mutants and addition of scavengers in partition system, to reveal the roles of catalase (CAT), photogenerated e^- and H_2O_2 in photocatalytic bacterial inactivation. A "parental strain" (*E. coli* BW25113) was more resistant than its isogenic single-gene deleted *katG*$^-$ mutant (*E. coli* JW3914) towards photocatalytic inactivation using TiO_2 irradiated by UVA lamps ($\lambda = 365$ nm) in a partition system, whereas the photocatalytic inactivation efficiency of both bacterial strains were similar in a non-partition system. Addition of scavengers and CAT demonstrated the importance of superoxide radical ($^{\bullet}O_2^-$), which subsequently formed H_2O_2, in the photocatalytic inactivation. The CAT activity and concentration of H_2O_2 during photocatalytic process were compared to further confirm the role of H_2O_2. In addition, bactericidal action of photogenerated e^- and pH effect on the photocatalytic inactivation inferred that H_2O_2 probably came from the conduction band of TiO_2. Furthermore, transmission electron microscope and atomic absorption spectrophotometric analyses indicated the oxidative damage of the bacterial cell began from cell envelope. The results of genetic and physiological analysis in this study provide a new insight into the cellular defense mechanism(s) during the photocatalytic inactivation of *E. coli*.

1. Introduction

Photocatalysis is a promising technique for water purification. TiO_2–UV is the most investigated photocatalytic system which is able to effectively degrade and detoxify a variety of organic and inorganic compounds [1]. The earliest study of the application of TiO_2 photocatalysis in microbial inactivation was reported by Matsunaga et al. [2] in 1985. Since then, TiO_2 photocatalytic inactivation of microorganisms has been studied extensively [3–9]. Although many studies investigated the modification and application synthetic photocatalysts [7,10–11], few of them reported the mechanism of photocatalytic inactivation [12,13]. In addition, the roles of bacterial cellular components and reactive oxidative species (ROSs) in photocatalytic bacterial inactivation have not been well-established.

Hydroxyl radical ($^{\bullet}OH$), either on photocatalyst surface (i.e., $^{\bullet}OH_{ads}$) or in bulk solution (that is $^{\bullet}OH_{free}$), has been widely reported as the major ROSs responsible for the inactivation of microorganisms or degradation of organic pollutants in both UV-irradiated TiO_2 and non-TiO_2 based UV or visible light (VL) photocatalytic systems [4,13–16]. However, recent studies have shown that other ROSs, such as H_2O_2, also involve in visible-light-driven (VLD) non-TiO_2 based photocatalytic inactivation [17]. Some studies even reported bactericidal activities of photo-generated electrons (e^-) in photocatalytic bacterial inactivation systems [17–19]. Nevertheless, the roles of superoxide ($^{\bullet}O_2^-$) and H_2O_2 have not been fully elucidated in TiO_2–UV system.

It is generally believed that photocatalytic bacterial inactivation begins with the damage of cell envelop (cell membrane and cell wall) by the photogenerated ROSs, followed by leakage of intracellular components, and finally leads to cell death. Moreover, different bacterial species produces different intracellular oxidative protective enzyme(s) results in different susceptibilities towards the attack of ROSs arising from photocatalysis [20]. A negative relationship between intracellular superoxide dismutase (SOD) activity and cell death was established, that is, photocatalytic inactiva-

* Corresponding author. Fax: +86 20 85290706.
** Corresponding author. Fax: +852 2603 5767.
E-mail addresses: antc99@gig.ac.cn (T. An), pkwong@cuhk.edu.hk (P.K. Wong).
[1] Equal contribution.

http://dx.doi.org/10.1016/j.cattod.2015.11.021
0920-5861/

tion efficiency decreased with an increase of initial SOD activity [21]. In addition, higher SOD and CAT activities imply higher tolerance of bacterial cells to ROSs generated from photocatalysis [22]. Besides, other cellular responses, such as degradation of endotoxin, peroxidation of phospholipid, leakage of potassium ion (K^+), and release of protein and nucleic acid were also observed in photocatalytic inactivation [12,23–25]. Unfortunately, most of these studies have only focused on the measurement of ultimate bactericidal results, and they generally have not considered the process(es) of bacterial stress responses during the photocatalytic inactivation. In particular, very few systematic and comparative studies have been reported on photocatalytic inactivation of a series of isogenic bacterial strains [26–28]. Thus, it is of great interest to reveal the bacterial cellular responses and their corresponding relevant photo-generated ROSs during the photocatalytic inactivation.

The present work studied the photocatalytic inactivation of *Escherichia coli* BW25113 (a "parental strain") and its isogenic single-gene deletion mutant, *E. coli* JW3914 (*katG*$^-$ mutant) using a TiO_2–UV system. A recently developed partition system was employed to separate the photocatalysts from bacterial cells to study the role of "direct contact" between photocatalysts and bacterial cells in photocatalytic inactivation. The different intracellular responses of the two bacterial strains towards different ROSs during the photocatalytic treatment were compared, and the protective roles of CAT and bactericidal action of photogenerated e^- and H_2O_2 were proposed. The use of different *E. coli* strains and partition system in this study can provide better understanding to the role fundamental defense mechanism of *E. coli* towards photocatalytic inactivation.

2. Materials and methods

2.1. Bacterial strains

E. coli BW 25113, a parental strain, and its single-gene deletion *katG*$^-$ mutant, *E. coli* JW3914, carrying the mutation of *katG729(del)::kan*, encoding catalase-peroxidase hydroperoxidase I (HP I) were selected in this study. Both bacterial strains were purchased from the Coli Genetic Stock Center (CGSC, Yale University, New Haven, CT, USA). The bacterial cells were cultured in Nutrient Broth (NB, Biolife, Milano, Italy) and harvested at stationary phase according to our previous study [26]. The composition of NB is as follows: Beef extract: 3.0 g/L, peptone: 5.0 g/L.

2.2. Photocatalytic performance

Detailed experimental procedures of photocatalytic inactivation were described in our previous studies [22,26]. Briefly, in the non-partition system, photocatalytic inactivation was conducted in a reactor as shown in Fig. S1a. In the partition system (Fig. S1b), 10 mL of *E. coli* 2×10^5 colony forming unit/mL (cfu/mL) in sterilized saline solution was pipetted into a semi-permeable membrane container. Outside of the membrane container was 30 mL sterile saline (0.9% NaCl) solution containing 100 mg/L TiO_2 (P25, Degussa Corporation, Germany). The light intensity of UVA irradiation (λ = 365 nm, 15 W, 60 Hz, Cole-Parmer, USA) was measured by an UVX digital radiometer (UVP, Inc., Upland, CA, USA) and fixed at 0.42 mW/cm^2. A magnetic stirrer was used to provide satisfactory mixing of the reacting solution. All glass apparatus used in the experiments were autoclaved at 121 °C for 20 min to ensure sterility, and all experiments in this study were performed in triplicates.

2.3. Scavenger study and partition system

The scavenger experiments were conducted by adding individual scavenger to quench respective ROSs into reaction mixture. Isopropanol [$(CH_3)_2CHOH$], potassium dichromate [$K_2Cr_2O_7$(Cr(VI))] and sodium oxalate ($Na_2C_2O_4$) were purchased from Riedel-deHaën Chemical Co., Germany, while ferric sulfate-ethylenediamine-tetraacetic acid [$FeSO_4$-EDTA(Fe(II))] was obtained from Ajax Chemicals, Australia. 4-Hydroxy-2,2,6,6-tetramethyl-piperidinyloxy (TEMPOL) was purchased from Sigma Chemical Co., USA. The applied concentration of each scavenger was optimized to ensure maximal scavenger effect with minimal toxicity to the bacterial cells [18]. The concentration of different scavengers used in this study is shown in Table 1. Catalase (CAT) was obtained from Cayman Chemical Company (Ann Arbor, MI, USA), and all of the chemicals were of analytical reagent grade except isopropanol which was of HPLC grade and dehydrated. Pure argon (≥99.995% (v/v), Hong Kong Oxygen & Acetylene Co., Ltd.) was used to purge into the reaction solution to produce an anaerobic condition.

Table 1
Concentrations of different scavengers used and their corresponding target ROSs.

Scavengers	Concentration (mM)	Target ROSs
Isopropanol	0.5	$^{\bullet}OH_{free}$
Potassium dichromate	0.05	e^-
Sodium oxalate	0.5	h^+
Fe-EDTA	0.1	H_2O_2
TEMPOL	2	$^{\bullet}O_2^-$

To study the importance of contact between the photocatalyst and bacterial cells in the photocatalytic inactivation, bacterial inactivation was conducted in a partition system [13]. In the partition system, a semi-permeable membrane was used to separate the photocatalyst and bacterial cells. Only ROSs that are long lasting and stable (that is H_2O_2) would be able to pass through the membrane and inactivate the bacterial cells. Therefore, the role of H_2O_2 in the system on bacterial inactivation can be further revealed.

2.4. Measurement of bacterial CAT activity and H_2O_2

The CAT activity was determined following the instruction protocol of a CAT Assay Kit (Cayman Chemical Company, Ann Arbor, MI, USA), and H_2O_2 was fluorescently measured by using the method reported by Abbas et al. [29].

2.5. Transmission electron microscopy

The untreated and photocatalytically treated bacterial cells were collected and centrifuged. Harvested cells were first prefixed by 2.5% glutaraldehyde and post-fixed by 1% osmium tetraoxide (E.M. grade, Electron Microscopy Sciences, Fort Washington, PA, USA). The stained ultra-thin 65 nm sections were examined under a Hitachi H-7650 transmission electron microscope (Tech comp Ltd., Tokyo, Japan). For detailed sample preparation, refer to our previous studies [30].

2.6. Measurement of K^+ leakage

To investigate K^+ leakage from the bacterial cells during the photocatalytic inactivation process, TiO_2 and bacterial cells in the suspension before and after photocatalytic treatment were harvested by centrifugation, and then the supernatant was used to measured K^+ concentration by a polarized Zeeman atomic absorption spectrophotometer (AAS) (Hitachi Z-2300, Tokyo, Japan).

3. Results

3.1. Photocatalytic performance

The photocatalytic inactivation efficiency of the parental strain and the *katG*⁻ mutant (Fig. S1) showed negligible decrease in bacterial cells population in the control experiments, indicating no toxic effect of TiO_2 (dark control) and UVA photolysis (light control) to the bacterial cells. When TiO_2 was irradiated by UVA, it exhibited high photocatalytic activity to inactivate bacterial cells. There were 7.5 log reduction of *E. coli* cells after 40 min irradiation.

3.2. Scavenger study

To reveal the role of different ROSs in photocatalytic bacterial inactivation, comparison experiments with the presence of different scavengers was conducted. As shown in Fig. 1, without the addition of any scavenger, complete photocatalytic inactivation of bacterial cells was achieved within 40 min treatment. With the addition of isopropanol as a scavenger for $^{\bullet}OH_{free}$, no inhibitory effect was observed for the bacterial inactivation. Notably, with the addition of H_2O_2 scavenger (that is, Fe(II)) and e^- scavenger (i.e., Cr(VI)), the photocatalytic bacterial inactivation was greatly inhibited for both the parental and *katG*⁻ mutant strains. The cell population only decreased less than 2 log for both bacterial strain. Interestingly, in the presence of TEMPOL to remove $^{\bullet}O_2^-$, the cell population of the parental strain decreased about 1 log (Fig. 1a), but the cell population of *katG*⁻ mutant remained unchanged during the inactivation processes (Fig. 1b). Although TEMPOL may also remove $^{\bullet}OH$ as well, the addition of $^{\bullet}OH$ scavenger showed no significant inhibition (Fig. 1). Therefore, the decrease of bacterial inactivation efficiency by TEMPOL should be due to the removal of $^{\bullet}O_2$. To further demonstrate the role of $^{\bullet}O_2^-$, an anaerobic experiment was conducted. With the purging of argon into the reaction solution to prevent the formation of $^{\bullet}O_2^-$, photocatalytic activity clearly reduced, and the population of *katG*⁻ mutant strain also decreased more slowly. With the addition of oxalate as a scavenger for h^+, the inactivation efficiency moderately decreased for both bacterial strains.

To further explore the role of e^-, oxalate was added to remove h^+ under anaerobic condition (that is, purging with argon). Under this condition, only e^- should remain in the system. The results show that in the first 20 min, the presence of e^- alone resulted in 3 and 2 log reduction of the cell population for the parental strain and the *katG*⁻ mutant, respectively (Fig. 1c). The populations of both bacterial strains did not decrease further when Cr(VI) was added at 20 min to remove e^- (Fig. 1c).

3.3. Contribution of H_2O_2

The effect of addition of CAT on the photocatalytic inactivation efficiency in the non-partition system is shown in Fig. 2. With increase of CAT concentration, the inhibition effect on photocatalytic bacterial inactivation increased (Fig. 2a). To further investigate the role of CAT, the effect of addition of CAT in the partition system was also conducted (Fig. 2b). The cell density of parental strain did not change in the dark and light controls, even after 6 h incubation. When the photocatalytic reaction occurred, the cell population of parental strain showed about 1.5 log reduction. On the contrast, for the katG⁻ mutant, in spite of the negligible toxicity of TiO_2, photolysis of the katG⁻ mutant in light control caused about 1.5 log cell reduction. Moreover, the cell population of katG⁻ mutant decreased by nearly 4 log during the photocatalytic treatment, and these results indicate that the katG⁻ mutant is more sensitive towards photocatalytic inactivation than the parental strain. When CAT was added into the partition system, the photo-

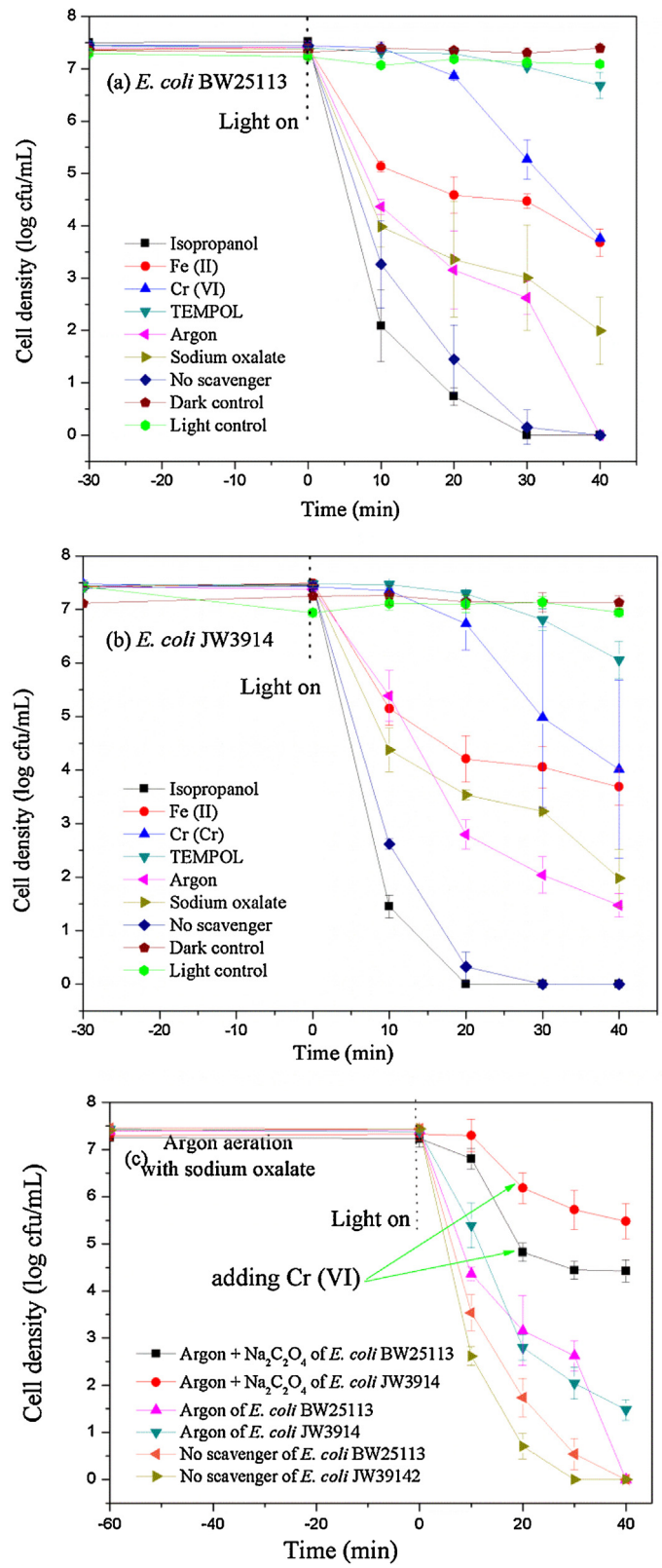

Fig. 1. Photocatalytic inactivation efficiency of (a) *E. coli* BW25113 and (b) *E. coli* JW3914 with different scavengers (0.5 mM isopropanol, 0.1 mM Fe(II)-EDTA, 0.05 mM Cr(VI), 2 mM TEMPOL, 0.5 mM $Na_2C_2O_4$). (c) *E. coli* BW25113 and *E. coli* JW3914 with the addition of 0.5 mM $Na_2C_2O_4$ and 0.05 mM Cr(VI) under anaerobic conditions. Pure argon was purged into the reaction mixture to eliminate oxygen. Error bars represent the standard deviation of 3 independent replicates.

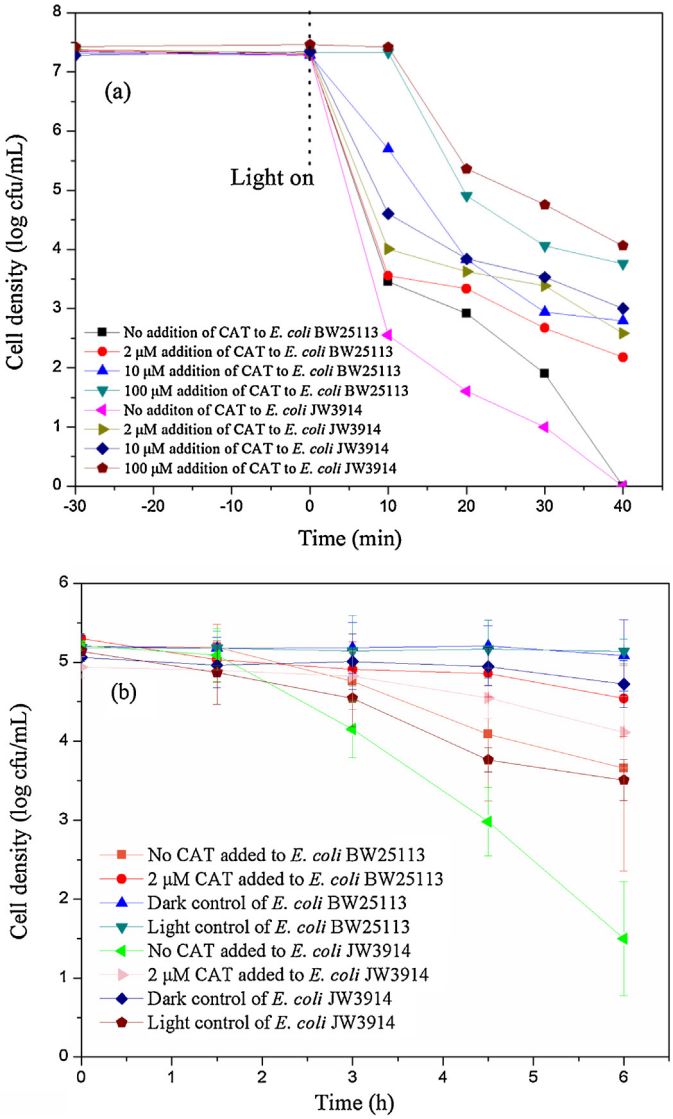

Fig. 2. Photocatalytic inactivation efficiency of *E. coli* BW25113 and *E. coli* JW3914 (a) with addition of different concentrations of CAT in non-partition system and (b) with and without addition of CAT in the inner compartment of the partition system. Error bars represent 3 independent replicates.

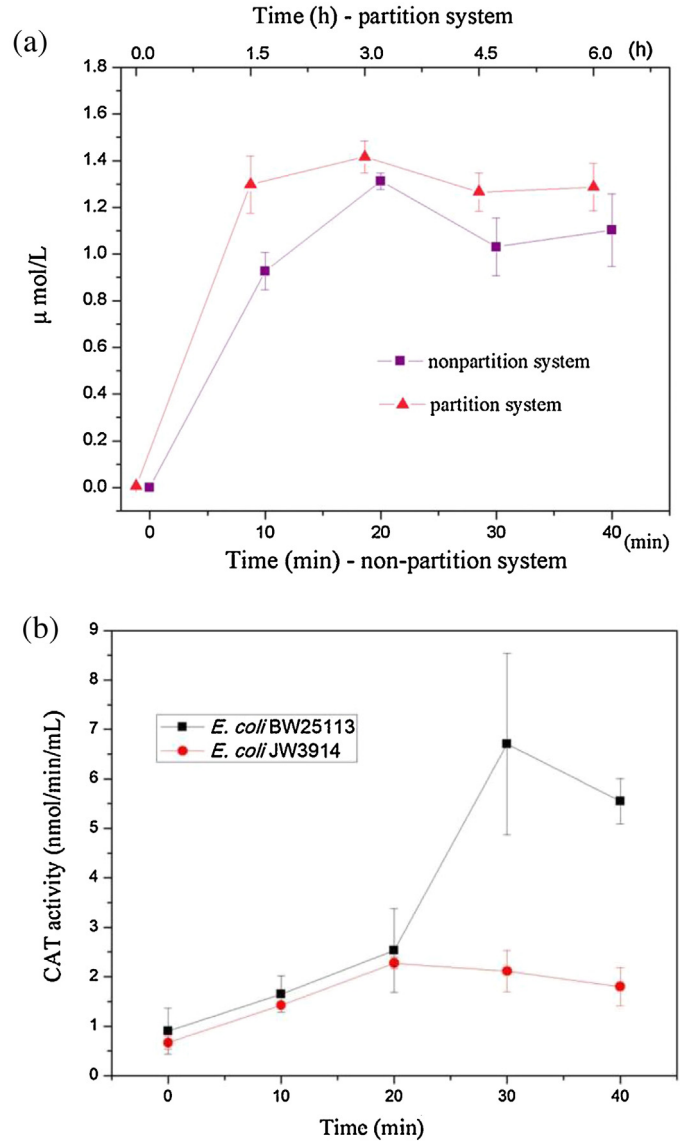

Fig. 3. (a) The H_2O_2 measurement against the illumination time both in the non-partition and partition systems. (b) Induction of CAT activity under the photocatalytic inactivation of *E. coli* BW25113 and *E. coli* JW3914 by TiO_2 under UV irradiation. Error bars represent the standard deviation of 3 independent replicates.

catalytic inactivation was almost completely inhibited (Fig. 2b). The production of H_2O_2 was detected in both the non-partition and partition systems. The H_2O_2 concentration increased rapidly in the first 10 min, and after 20 min, it reached an equilibrium concentration around 1.1 μM (Fig. 3a).

3.4. Bacterial CAT activity

To further confirm the attack of bacterial cells by H_2O_2, the bacterial CAT activity during the photocatalytic inactivation was measured in the parental and *katG*⁻ mutant strains. As shown in Fig. 3b. For the parental strain, the CAT activity increased rapidly with time in the initial 30 min, and the maximum CAT activity was detected at 30 min which was about 5 times higher than that at the beginning of the photocatalytic inactivation. After 30 min treatment, the CAT activity began to decrease. However, the *katG*⁻ mutant did not show such a significant CAT inducible process. The residual CAT activity that appeared in *katG*⁻ mutantwas mainly due to the expression of another catalase (KatE) by the mutant.

3.5. pH effect

To further investigate the role of H_2O_2, the pH effect on the photocatalytic inactivation was conducted both in the non-partition and partition systems (Fig. S2). Compared with neutral pH, the photocatalytic inactivation efficiency was greatly increased at acidic pH (4.0) and reduced at alkaline pH (8.5). There was a slight reduction (about 1 log) in the non-partition system due to adsorption between the bacterial cells and photocatalysts (Fig. S2a), while, in the partition system, there is no reduction in the cell population because the bacterial cells and photocatalysts were separated. Thus, the bacterial cells did not change in dark controls and light controls within 3 h, which suggests the bacterial cell can survive under both acidic and alkaline conditions. However, the bacterial cells can be completely inactivated within 3 h in photocatalytic system at pH 4.0 when the light was applied. While at pH 6.8 and 8.5, the population of bacterial cells almost did not change within 3 h under the same photocatalytic treatment (Fig. S2b).

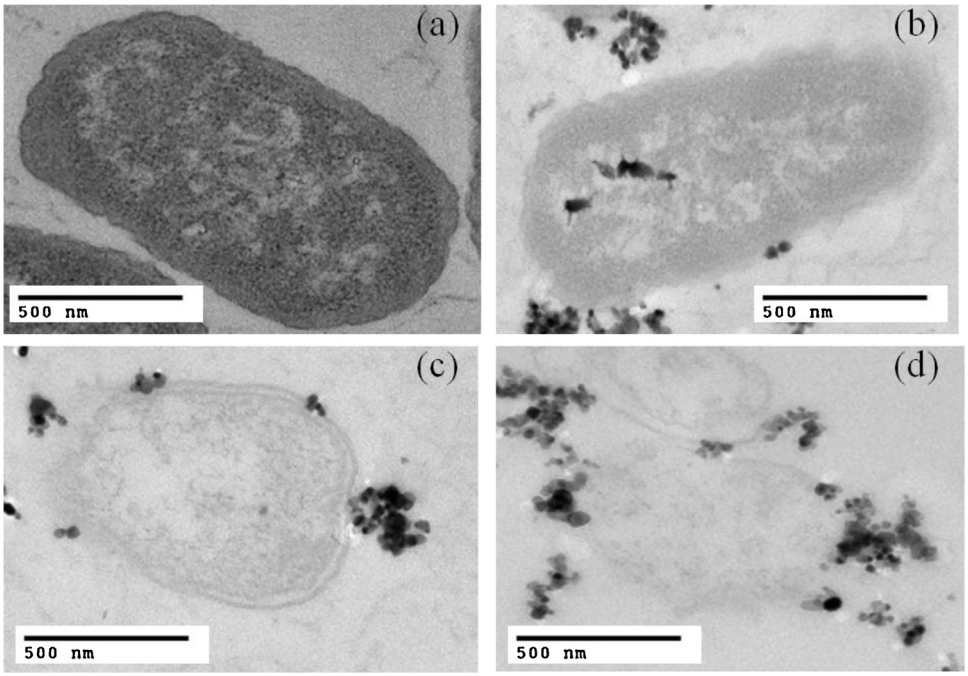

Fig. 4. TEM images of *E. coli* BW25113 before and after photocatalytically treatment with TiO_2 under UV irradiation. (a) 0 h, (b) 1 h, (c) 3 h and (d) 6 h.

3.6. Destruction model of bacterial cells

To elucidate the destruction process of bacterial cells in the H_2O_2 dominant photocatalytic system, the structure and morphology of *E. coli* BW25113 before and after photocatalytic treatment were examined by transmission electron microscopy (TEM) (Fig. 4). Before photocatalytic inactivation, the bacterial cells exhibited a rod-shaped morphology with a good preservation of the cellular structure. A smooth and continuous cell envelope (cell wall and cell membrane) surrounded the cytoplasm, indicating a well-defined cell wall and cell membrane (Fig. 4a). After 1 h treatment, the bacterial cells showed some morphological damages with obviously obscured and disorganized cell membrane (Fig. 4b). After 3 h treatment, the bacterial cells showed abnormally wavy cell envelope and lost most of their intracellular contents (Fig. 4c). Eventually, the bacterial cell wall was completely damaged and ruptured, the entire part of the membrane was missing and the cytoplasmic contents were released (Fig. 4d). These results indicate that the destruction process of the cells begins from cell envelope towards intracellular components. Potassium ion (K^+), a major cation of intracellular fluids in bacterial cells involved in the regulation of polysome content and protein synthesis, quickly leaked out from the bacterial cells during the inactivation process (Fig. S3) because of the significant damage in cell membrane by the photocatalytic treatment [31].

4. Discussion

E. coli, a common waterborne bacterium, with the best-studied genetics and the largest number of mutants, was chosen as a model microorganism to investigate the photocatalytic inactivation in this study. The *katG*$^-$ mutant (*E. coli* JW3914) is a isogenic single-gene deletion mutant derived from the parental strain (*E. coli* BW25113), and both strains belonged to the Keio collection [32], which can enable us to determine the role of intracellular enzyme, catalase (CAT), of the bacteria in photocatalytic inactivation. Fig. S4 compares the photocatalytic inactivation efficiencies of the parental and katG$^-$ mutant strains in the TiO_2–UVA system. The results indicated that the *katG*$^-$ mutant is slightly susceptible than the parental strain towards photocatalytic inactivation in non-partition system; notably, the *katG*$^-$ mutant is much more sensitive than the parental strain in partition system (Fig. 2b). The different susceptibilities of these two bacterial strains towards photocatalytic inactivation are probably due to the only genetic difference, which will be further discussed below.

In order to clarify the contribution of different photogenerated ROSs and the correlation between ROSs and bacterial responses during photocatalytic inactivation, a series of scavenger addition experiments were conducted. Based on the difference of the inactivation efficiency in the presence of different scavengers, it can clarify the roles of different ROSs in this photocatalytic system. Addition of isopropanol in the system shows that diffusing $^{\bullet}OH_{free}$ is not directly involved in bacterial inactivation in this TiO_2–UV photocatalytic system, which is quite different from previous studies [4,13–16]. It is probably due to the use of different bacterial strains, thus different responses were obtained towards photogenerated ROSs. On addition of Fe(II) and Cr(VI), the photocatalytic inactivation activity was greatly inhibited. It suggests that H_2O_2 is one of the major ROSs involved in bacterial inactivation in the system. In addition, comparing Fig. 1a–c, most of the inactivation efficiencies after the addition of scavengers on the parental and *katG*$^-$ mutant strains are almost the same, except the purging of argon into the system (Fig. 1c). In the absence of O_2 by purging with argon, no $^{\bullet}O_2^-$ is produced and only e^- is remained, thus only e^- and H_2O_2 produced by the valence band were able to inactivate bacterial cells (Fig. 1c).

On the other hand, oxalate is an excellent scavenger for suppressing direct h^+ oxidation, because oxalate shows strong affinity onto photocatalyst surface. Thus, $^{\bullet}OH_{ads}$ produced by h^+ will be reduced in the presence of oxalate. The experiment of addition of oxalate under anaerobic conditions (that is purging argon) further demonstrates that the reductive site (e^-) is significantly involved in the photocatalytic inactivation. In the presence of oxalate and argon, the formation of ROSs from both valence and conduction band were inhibited, then only e^- remained to inactivate bacterial cells (Fig. 1c). The results in the present study suggest that e^-,

and H_2O_2, are the major ROSs responsible for the photocatalytic inactivation in this TiO_2–UV system.

To further confirm the role of H_2O_2, CAT was added in the partition system, in which photocatalysts and bacterial cells were separated. CAT catalyzes the decomposition of H_2O_2 to water and oxygen [33], which largely contributes to the protection of cells from excess oxidative stress. Inhibition effect of adding CAT to the photocatalytic bacterial inactivation in the partition system indicates the significant contribution of H_2O_2 towards the photocatalytic bacterial inactivation (Fig. 2).

Furthermore, the semi-permeable membrane in the partition system only allows diffusing species such as $^{\bullet}OH_{free}$ and H_2O_2 to enter the inner compartment with bacterial suspension. In fact, it is conceivable that the "half-length" of $^{\bullet}OH$ [34], referring to its half-life of nanoseconds, is limited to a few μm in solution. Therefore, theoretically, it is impossible for $^{\bullet}OH_{free}$ to transport across the semi-permeable membrane with a thickness of 25–50 μm [6]. There are several reports suggesting that $^{\bullet}OH$ cannot permeate through cell membranes [35], whereas H_2O_2 is able do so [36]. Thus, the addition of CAT in the partition experiments demonstrated the crucial role of H_2O_2 in this photocatalytic bacterial inactivation.

Based on the above scavenger studies, the major bactericidal species is not $^{\bullet}OH_{free}$, but H_2O_2. It has been well known that, H_2O_2 has two modes of bactericidal action: Mode I occurs at lower H_2O_2 concentration less than 2 mM which can damage DNA and is independent with the concentration of H_2O_2, while Mode II occurs at H_2O_2 concentration greater than 10 mM and involved the formation of $^{\bullet}OH$ through Fenton reaction [10,37,38]. However, in this study, only μM level of H_2O_2 was detected during the photocatalysis, and this concentration falls in the lower range for Mode I inactivation. But H_2O_2 is continuously produced and depleted dynamically, this implies that the total amount of H_2O_2 in the system should reach a dynamic equilibrium.

Furthermore, the pH effect was examined both in the non-partition and partition systems to determine the contribution of the reductive photocatalytic pathways. In the conduction band of TiO_2, e^- first reacts with oxygen (O_2) to form $^{\bullet}O_2^-$, which further reacts with proton (H^+) to form hydroperoxyl radical ($^{\bullet}HO_2$) and H_2O_2; on the other hand, the valence band-h^+ can react with water or hydroxyl anion (OH^-) to generate $^{\bullet}OH_{free}$, then to form H_2O_2 because of short half-life, as shown below:

$$O_2 \xrightarrow{e^-} {}^{\bullet}O_2^- \overset{H^+}{\rightleftharpoons} {}^{\bullet}HO_2 \xrightarrow{H^+, e^-} H_2O_2 \quad (1)$$

$$h^+ \xrightarrow{H_2O/OH^{\bullet}} Oh_{adsorfree} \rightarrow H_2O_2 \quad (2)$$

In the partition system, the bacterial cells and photocatalyst are separated, which prevents the adsorption between the bacterial cells and photocatalysts. Under acidic condition, $^{\bullet}O_2^-$ can react with more H^+, therefore, more H_2O_2 was produced from the conduction band (Eq. (1)). The great enhancement of photocatalytic inactivation was achieved at pH 4.0 (Fig. S2), which is mainly due to the higher accumulation of permeable H_2O_2 produced from the conduction band of TiO_2 in the presences of higher concentration of H^+. The results suggests that the H_2O_2 coming from the sequential reactions of conduction band is probably one of the major ROS to inactivate bacterial cells in the present system. On the contrary, more H_2O_2 was produced from the valence band of TiO_2 under alkaline condition (Eq. (2)).

During the photocatalytic reaction, the bacterial defense system induces higher level of CAT in order to mitigate the oxidative attack of H_2O_2. Therefore, increase of CAT activity implies a stronger H_2O_2 attack encountered by the bacterial cells during photocatalytic process. After 30 min treatment, the CAT activity began to decrease, suggesting the oxidative stress from H_2O_2 and other ROSs generated by TiO_2–UV exceeds the protection ability of the bacterial oxidative defense system, leading to the loss of bacterial viability. However, the change of CAT activity of the *katG*⁻ mutant was not as significant as compared with that of the parental strain. The *katG* gene encodes CAT-HP I which possesses both catalase and peroxidase activity, and mutations in katG will prevent the formation of both CAT-HP I and isoenzyme forms of the bifunctional CAT [39–41]. Thus, it is postulated that, due to the difference in genetic properties of the two bacterial strains, they display different sensitivities to H_2O_2 in the photocatalytic system. Finally, the experiments of TEM images and K^+ leakage demonstrate the destructive process starting from cell envelope of bacterial cells.

In general, $^{\bullet}OH$ is believed to be the major ROSs responsible for the inactivation of bacteria [42]. The low concentration of H_2O_2 that was produced in common photocatalytic system (usually <60 μM) should be unable to effectively inactive bacterial cell [43] and not contribute much in photocatalytic bacterial inactivation system. The results of this study showed that the low concentration of H_2O_2 can also play important roles in the photocatalytic bacterial inactivation. Therefore, the role of other ROSs in photocatalytic bacterial inactivation systems should be investigated as well in order to fully understand the mechanisms of photocatalytic inactivation.

5. Conclusions

In conclusion, the present study provides a new aspect to study the roles of ROSs and the corresponding bacterial cellular changes during the photocatalytic inactivation by combining two approaches: usage of genetic (mutants), and chemical (scavenger) and biochemical (catalase activity) to reveal the important role of catalase in the photocatalytic bacterial inactivation. The parental and mutant strains show different sensitivity towards photocatalytic inactivation. Moreover, the physiological responses of parental and mutant strains are compared. Traditionally, $^{\bullet}OH$ is regarded as the major ROS that responsible for the bacterial inactivation in TiO_2/UVA system. However, the results of this study also indicate that other ROSs, such as e^- and H_2O_2, are also involved in the bacterial inactivation processes. Therefore, the role of other ROSs in the photocatalytic inactivation should not be underestimated. The combination of bacterial mutants, chemical scavenger studies and biochemical enzyme assay tests used in this study provide a new approach for the investigation of photocatalytic inactivation mechanism.

Acknowledgements

The project was supported by a research grant (General Research Fund 476811) of the Research Grant Council, Hong Kong SAR Government to P.K. Wong and NSFC grant (41425015 and 41573086) to T.C. An and G.Y. Li. Prof. P.K. Wong was also supported by CAS/SAFEA International Partnership Program for Creative Research Teams. The authors also thank Mr. Freddie Kwok of the Chinese University of Hong Kong for the technical assistance in TEM study.

Appendix A. Supplementary data

Supplementary data associated with this article can be found, in the online version, at http://dx.doi.org/10.1016/j.cattod.2015.11.021.

References

[1] A. Fujishima, T.N. Rao, D.A. Tryk, J. Photochem. Photobiol. C: Photochem. Rev. 1 (2000) 1–21.
[2] T. Matsunaga, R. Tomoda, T. Nakajima, H. Wake, FEMS Microbiol. Lett. 29 (1985) 211–214.
[3] M. Cho, H. Chung, W. Choi, J. Yoon, Appl. Environ. Microbiol. 71 (2005) 270–275.

[4] G. Gogniat, S. Sam Dukan, Appl. Environ. Microbiol. 73 (2007) 7740–7743.
[5] J.C. Ireland, P. Klostermann, E.W. Rice, R.M. Clark, Appl. Environ. Microbiol. 59 (1993) 1668–1670.
[6] Y. Kikuchi, K. Sunada, T. Iyoda, K. Hashimoto, A. Fujishima, J. Photochem. Photobiol. A: Chem. 106 (1997) 51–56.
[7] D.S. Kim, S.Y. Kwak, Environ. Sci. Technol. 43 (2009) 148–151.
[8] K.P. Kühn, I.F. Chaberny, K. Massholder, M. Stickler, V.W. Benz, H.G. Sonntag, L. Erdinger, Chemosphere 53 (2003) 71–77.
[9] L. Rizzo, J. Hazard. Mater. 165 (2009) 48–51.
[10] S. Ge, L. Zhang, Environ. Sci. Technol. 45 (2011) 3027–3033.
[11] C. Pan, Y. Zhu, Environ. Sci. Technol. 44 (2010) 5570–5574.
[12] P.C. Maness, S. Smolinski, D.M. Blake, Z. Huang, E.J. Wolfrum, W.A. Jacoby, Appl. Environ. Microbiol. 65 (1999) 4094–4098.
[13] L.S. Zhang, K.H. Wong, H.Y. Yip, C. Hu, J.C. Yu, C.Y. Chan, P.K. Wong, Environ. Sci. Technol. 44 (2010) 1392–1398.
[14] M. Cho, H. Chung, W. Choi, J. Yoon, Water Res. 38 (2004) 1069–1077.
[15] S. Kim, W. Choi, Kinetics and mechanisms of photocatalytic degradation of $(CH_3)\ nNH_4\text{-}n+(0 \le n \le 4)$ in TiO_2 suspension: the role of OH radicals, Environ. Sci. Technol. 36 (2002) 2019–2025.
[16] J. Peller, O. Wiest, P.V. Kamat, J. Phys. Chem. A 108 (2004) 10925–10933.
[17] Y.M. Chen, A.H. Lu, Y. Li, L.S. Zhang, H.Y. Yip, H.J. Zhao, T.C. An, P.K. Wong, Environ. Sci. Technol. 45 (2011) 5689–5695.
[18] W.J. Wang, L.S. Zhang, T.C. An, G.Y. Li, H.Y. Yip, P.K. Wong, Appl. Catal. B: Environ. 108–109 (2011) 108–116.
[19] W.J. Wang, J.C. Yu, D.H. Xia, P.K. Wong, Y.C. Li, Environ. Sci. Technol. 47 (2013) 8724–8732.
[20] H.A. Foster, I.B. Ditta, S. Varghese, A. Stelle, Appl. Microbiol. Biotechnol. 90 (2011) 1847–1868.
[21] Y. Koizumi, R. Yamada, M. Nishioka, Y. Matsumura, T. Tsuchido, M. Taya, J. Chem. Tech. Biotechnol. 77 (2002) 671–677.
[22] T.Y. Leung, C.Y. Chan, C. Hu, J.C. Yu, P.K. Wong, Water Res. 42 (2008) 4827–4837.
[23] J. Kiwi, V. Nadtochenko, Langmuir 21 (2005) 4631–4641.
[24] K. Sunada, Y. Kikuchi, K. Hashimoto, A. Fujishima, Environ. Sci. Technol. 32 (1998) 726–728.
[25] H. Sun, G. Li, X. Nie, H. Shi, P.K. Wong, H. Zhao, T. An, Environ. Sci. Technol. 48 (2014) 9412–9419.
[26] M.H. Gao, T.C. An, G.Y. Li, X. Nie, H.Y. Yip, H.J. Zhao, P.K. Wong, Water Res. 46 (2012) 3951–3957.
[27] R. Hong, T.Y. Kang, C.A. Michels, N. Gadura, Appl. Environ. Microbiol. 78 (2012) 1776–1784.
[28] X. Shi, G. Huang, D. Xia, T.W. Ng, H.Y. Yip, G. Li, T. An, H. Zhao, P.K. Wong, J. Phys. Chem. B 119 (2015) 3104–3111.
[29] M.E. Abbas, W. Luo, L. Zhu, J. Zou, H. Tang, Food Chem. 120 (2010) 327–331.
[30] Y.W. Cheng, R.C.Y. Chan, P.K. Wong, Water Res. 41 (2007) 842–852.
[31] C. Ren, W.Z. Wang, L. Zhang, J. Chang, H. Sheng, Catal. Commun. 10 (2009) 1940–1943.
[32] T. Baba, T. Ara, M. Hasegawa, Y. Takai, Y. Okumura, M. Baba, K.A. Datsenko, M. Tomita, B.L. Wanner, H. Mori, Mol. Syst. Biol. 8 (2006) 1–11.
[33] M. Zamocky, F. Koller, Prog. Biophys. Mol. Biol. 72 (1999) 19–66.
[34] B.L. Triggs-Raine, P.C. Loewen, Gene 52 (1987) 121–128.
[35] M. Takahashi, K. Asada, Arch. Biochem. Biophys. 226 (1983) 558–566.
[36] G. Brandi, F. Cattabeni, A. Albano, O. Cantoni, Free Radic. Res. Commun. 6 (1989) 47–55.
[37] J.A. Imlay, S. Linn, J. Bacteriol. 166 (1986) 519–527.
[38] P.C. Loewen, B.L. Triggs, C.S. George, B.E. Hrabararchuk, J. Bacteriol. 162 (1985) 661–667.
[39] B.L. Triggs-Raine, B.W. Doble, M.R. Mulvey, P.A. Sorby, P.C. Loewen, J. Bacteriol. 170 (1988) 4415–4419.
[40] H.E. Schellhorn, FEMS Microbiol. Lett. 131 (1994) 113–119.
[41] R. Singh, B. Wiseman, T. Deemagarn, V. Jha, J. Switala, P.C. Loewen, Arch. Biochem. Biophys. 471 (2008) 207–214.
[42] M. Cho, H. Chung, W. Choi, J. Yoon, Water Res. 38 (2004) 1069–1077.
[43] M.D. Labas, C.S. Zalazar, R.J. Brandi, A.E. Cassano, Biochem. Eng. J. 38 (2008) 78–87.